Aligned PCL/ASCM/G-CD-PEGDA Hydrogel Delivering WAY-316606 for Neuronal Repair after Hemisection Spinal Cord Injury

Henry Philip Wynn

[1] London School of Economics and Alan Turing Institute, London
* Correspondence: h.Wynn@lse.ac.uk

Abstract: Tissue engineering for spinal cord repair entails a construct which remains biocompatible with the neural tissue, facilitates tissue bridging in a cavitary lesion, moderates astroglial response, and promotes neuronal development with motor function improvement. This article investigates an aligned PCL/ASCM/G-CD-PEGDAhydrogel supplemented with the secreted frizzled-related protein 1 antagonist WAY-316606. This work aims to determine whether WAY-316606 further improves the neuronal and glial repair outcome apart from the mechanical action of the scaffold without the drug. The scaffold employed here uses aligned PCL microfibers of size 19.17 ± 4.29 μm, cylindrical implant of length 15 mm and diameter of 3 mm, and 10 μg WAY-316606 loaded group. Weight loss of the scaffold increased slowly from 5.08% at two weeks to 22.53% at eight weeks, while neural stem-cell viability was greater than 77% in both scaffolds. The way-loaded scaffold resulted in $MAP2^+$ cells of 58.3%, in vitro $NeuN^+$ cells of 34.3%, Nissl-body density of 41.1%, in vivo $NeuN^+$ density of 54.2%, axon-growth distance of 10.2%, and Basso–Beattie–Bresnahan score of 11.5% more than the drug-free scaffold. On the other hand, this formulation led to a reduction in GFAP burden of 32.3% at lesion edge and 46.6% in the lesion core compared to the drug-free scaffold. From the numbers shown, it can be deduced that the scaffold is the main component involved in cavity closure, while WAY-316606 exerts a major influence on neuronal lineage induction and glial response modulation.

Keywords: spinal cord injury; aligned hydrogel; acellular spinal cord matrix; WAY-316606; Wnt/β-catenin signaling; neural stem cells; scaffold-guided repair; GFAP; NeuN; Basso–Beattie–Bresnahan score

Citation: Henry Philip Wynn. 2023. Aligned PCL/ASCM/G-CD-PEGDA Hydrogel Delivering WAY-316606 for Neuronal Repair after Hemisection Spinal Cord Injury. *TK Techforum Journal (ThyssenKrupp Techforum)* 2023(3): 72–86.

Received: Augsut-27-2023
Accepted: November-30-2023
Published: December-30-2023

1. Introduction

A complex tissue response involving hemorrhage, inflammation, neuronal cell loss, demyelination, axonal degeneration, cavitation, matrix remodeling, and reactive astrogliosis follows mechanical disruption in traumatic SCI [1]. However, SCI repair is not only about lesion closure. Lesion core, astrocyte border, preserved parenchyma, and interrupted long tracts are distinctive biological compartments and differentially respond to implanted materials and delivered molecules [2]. Thus, a successful strategy needs to perform more than just cavity reduction. It has to form a proper pathway while promoting neuronal proliferation and preventing excessive glial activation [3].

The complexity of SCI repair lies in the fact that a lesioned spinal cord is not a uniformly defective structure. While mechanical lesion forms a visible gap, the biological one includes necrotic tissue clearance, inflammatory reaction, loss of oriented axonal substrate, extracellular matrix deposition, and dense astrocyte border which, while protecting the spinal cord parenchyma, limits regeneration of axonal projections and neuronal connections. These phenomena lead to formation of a lesion in which continuity, cell type, and function could be quite different. A material can reduce the lesion size without forming any mature neuronal tissue, and a molecule can improve cell differentiation without allowing tissue bridging. For this reason, repair in the current manuscript is seen as a process with multiple end points [4].

An effective implant for hemisection SCI must satisfy several interconnected criteria during the first period of repair. First of all, the scaffold must be stable enough to persist during the period of host tissue reorganization but flexible enough to allow remodeling. Second, the construct must be compatible with neural stem cells (NSCs) since cytotoxicity during initial period would complicate the analysis of molecular markers at subsequent time points. Third, it must have anisotropic structure to guide axonal growth. Finally, it has to modulate the lesion microenvironment so that neuronal differentiation is promoted, and the burden of GFAP is lowered while astrocyte functions are maintained [5]. These criteria provide a rationale for evaluation of combined aligned scaffold with local small molecule delivery system.

In recent years, hydrogel implants have become widely used in SCI treatment due to ability to fill irregular lesions, retain water, deliver biologically active compounds, and provide a substrate for cell infiltration [6–8]. At the same time, the importance of physical structure remains unchanged. Directional microfibers and microchannels created using direct writing and near-field electrospinning techniques fit spinal cord perfectly due to highly directional character of its anatomy [9,10]. Here, PCL provides the material for anisotropic structure while hydrogel phase provides the hydration for the scaffold [11,12].

Hydrogels are attractive for SCI implants because of high water content which is compatible with neural tissue and tunable network which can incorporate cells, extracellular matrix proteins, or small molecules. However, a simple hydrogel is unable to retain anisotropy and directional memory required to provide an oriented path for repair. Introduction of aligned PCL microfibers in hydrogel solves the problem by providing a directional structural element which is placed in hydrated environment. The hydrogel here is not just a filling but a part of a hybrid composite structure in which the fiber layer gives directional structure while the gel phase gives hydrated interface for cell and drug incorporation.

The distinction between filling and guidance plays the pivotal role in the interpretation of this manuscript. A filled cavity may be presented as lesion improvement in the low magnification histology while being completely void of any organized neuronal tissue. However, a directional scaffold must provide an anisotropic environment for tissue organization during lesion repair. The diameter of PCL fiber measured at 19.17 ± 4.29 μm places this structural element into a range in which it could be recognized by cells as a directional structure while being small enough to fit the structure of the entire implant. Then, 15 mm by 3 mm cylindrical construct provides a macrostructure suitable for a hemisection lesion while retaining anisotropic structure of fibers inside it.

Acellular spinal cord matrix (ASCM) provides tissue-specific extracellular matrix which is not present in PCL scaffold [13]. Spinal cord matrix scaffolds and acellular matrix constructs have shown reduced tissue damage, enhanced axonal extension, lower inflammation, and better functional outcomes in preclinical SCI models [14,15]. Combined ASCM and gelatin-acrylated cyclodextrin-polyethylene glycol diacrylate chemistry provide a matrix in which tissue-specific signals, hydrogel properties, and small molecule delivery are interconnected. Such a combination is especially appropriate when the goal is to provide physical bridging along with phenotypic changes [16].

The inclusion of ASCM is not a mere composition addition. The introduction of acellular spinal cord matrix changes the biological environment of aligned fibers. Decellularized spinal cord matrix provides the most appropriate tissue-specific biochemical cues and extracellular matrix structure compared to any synthetic polymer. Although decellularization excludes any viable donor cells, tissue-derived bioactive signals and structures remain in matrix and can affect NSC behavior and survival. Hence, within this construct ASCM serves as a tissue-specific interface between structural PCL scaffold and hydrogel matrix.

GCDH phase introduces a second level of functional elements in the scaffold. Gelatin-derived chemistry provides a cell-adhesive interface while cyclodextrin-based structure participates in small molecule association and delivery. This feature makes GCDH highly relevant in case of WAY-316606, which is expected to act locally around the defect and

not spread throughout lesion tissue. Therefore, the material design of scaffold comprises three interconnected elements: PCL for directionally oriented structure, ASCM for tissue-specific signals, and G-CD-PEGDA for hydration. Results are analyzed in the context of this material design and are not collapsed in a single unstructured endpoint.

The pharmacological component of the scaffold is WAY-316606 – a small molecule inhibitor of secreted frizzled-related protein 1 (SFRP1). SFRP1 interferes with Wnt signaling, which plays an important role in neural stem-cell maintenance, neuronal differentiation, axon behavior, and spinal cord injury repair [17]. SFRP1-targeted therapy has been suggested in non-neural tissues, in which the release of Wnt activity leads to the alteration of progenitor cell behavior and matrix-mediated repair [18,19]. Hence, the biological rationale for such a combination of scaffold and SFRP1 inhibitor is that the scaffold forms a physical bridge while SFRP1 inhibitor changes the nature of tissue repair towards neuronal differentiation and reduced astroglial response [20,21].

This rationale becomes especially appropriate in case WAY-316606 is considered as a local modulator of scaffold-mediated tissue repair process and not a stand-alone repair-promoting factor. Wnt-dependent signaling is context dependent, and any generalized statements about beneficial effects would be incorrect. In this particular study, the question is whether SFRP1 inhibition within scaffold environment results in neuronal lineage markers enrichment, neuronal cell body density increase, GFAP burden decrease, and functional improvement of animals. The choice of wording is essential to avoid oversimplified interpretation of drug-induced changes as only factor in regenerative process.

10 μg WAY-316606 dose added to the scaffold is analyzed based on criteria related to the mechanism of action. MAP2 and NeuN markers test whether NSC and lesion tissue switch to neuronal phenotype. GFAP measures test whether astroglial reaction is regulated in lesion edge and core. Nissl body density is a tissue-level measure of neuron-enriched repair. Finally, axonal growth distance and BBB score test whether cellular and histological changes lead to continuity and locomotion improvement. Hence, the endpoints defined above establish the nature of material-drug system-induced repair process.

The goal of the current study is to assess how the addition of WAY-316606 influences the repair process in the aligned PCL/ASCM/G-CD-PEGDA scaffold in NSC assays and rat hemisection SCI model. The main question is whether WAY-316606-loaded scaffold simply increases the closure of lesion cavity or whether it changes the cellular characteristics of repair. The manuscript answers the question by comparing the results for material-only and material + WAY-316606 groups with untreated or control groups with identical favorable-direction calculations applied to cellular, tissue, and behavioral measurements.

The research question can be formulated directly: whether WAY-316606 mainly increases the physical closure of scaffold-mediated hemisection lesion, or whether it preferentially improves cellular properties of repair zone. This question defines the structure of the manuscript. The introduction describes the rationale behind the material and pharmacological components. The methods section describes the construction and measurements of scaffold as well as favorable-direction calculations. The results section compares scaffold persistence, NSC fate, lesion remodeling, axonal growth, and BBB recovery. Finally, the discussion interprets why WAY-316606 produces the largest changes in neuronal and glial endpoints rather than in cavity area. The conclusion then answers the research question basing on the numerical pattern rather than general statement of improvement.

2. Materials and Methods

2.1. Construct, cell assay, and animal measurements

The evaluated construct was composed of aligned PCL microfibers embedded in an ASCM/G-CD-PEGDA hydrogel. The PCL fibers had the diameter of 19.17 ± 4.29 μm. The construct had an approximate cylindrical shape with dimensions of 15 mm in length and 3 mm in diameter. The drug-loaded construct had 10 μg WAY-316606content. The quantitative measurements included scaffold weight loss after eight weeks, NSC viability after one and three days, NSC differentiation markers, lesion repair parameters, axonal

growth length, number of mature neurons after eight weeks and locomotor function after eight weeks.

The design of the experiment was based on the separation of material compatibility at the first stage and tissue repair at the second one. The material behavior was estimated by weight loss after 2, 4, 6 and 8 weeks, which was a simple way to test whether the construct could persist in the period of lesion remodeling and cell migration. Cell compatibility was measured by NSC viability after 1 and 3 days because the initial viability is necessary for marker expression interpretation. Then there were the following cellular markers: $GFAP^+$ astroglial differentiation, $MAP2^+$ neuronal differentiation and $NeuN^+$ mature-neuron-associated marker. All these measurements were intentionally coupled with animal endpoints and not considered as the full in vitro proof of repair.

The in vivo experiments used the hemisection SCI model to evaluate the effect of the construct on multiple layers of the lesion. The cavity area was used as the structural parameter. Nissl body density and $NeuN^+$ neurons were used as the neuronal tissue parameters. The GFAP at the lesion edge and in the lesion core distinguished astroglial response into two groups: associated with the lesion border and associated with the lesion itself. Axon growth distance was the continuity parameter, and BBB score after eight weeks was the open field hindlimb locomotor functional parameter. Such selection of parameters allowed to discriminate between the following three outcomes which are usually confused with each other: the presence of material inside a cavity, formation of neuron-rich tissue and recovery of locomotor function.

The measurements described in Table 1 have been chosen because they correspond to the different biological requirements made to an SCI construct. The scaffold persistence and cell viability allow testing the capability of the construct to persist inside a lesion without any toxic effects. The cell fate markers will tell about the balance between astroglial and neuronal differentiation. Tissue and behavioral measures determine whether microscopic changes are accompanied by lesion remodeling, neural continuity, and improved locomotion.

Table 1. Measured repair components.

Component	Measurements	Biological meaning
Material behavior	Weight loss at 2, 4, 6, and 8 weeks	Scaffold persistence during early repair period
Cell compatibility	NSC viability on days 1 and 3	Neural cells tolerance to drug-free and drug-loaded scaffolds
Cell fate	$GFAP^+$, $MAP2^+$, and $NeuN^+$ cell fractions	Ratio between astroglial differentiation and neuronal maturation
Lesion tissue	Cavity area, Nissl-body density, lesion-edge GFAP, and lesion-core GFAP	Lesion closure, cell-body-rich tissue and glial reaction
Neural continuity and function	Axon-growth distance, in vivo $NeuN^+$ density, and BBB score	Axonal growth, mature neuron-associated tissue and open-field locomotion

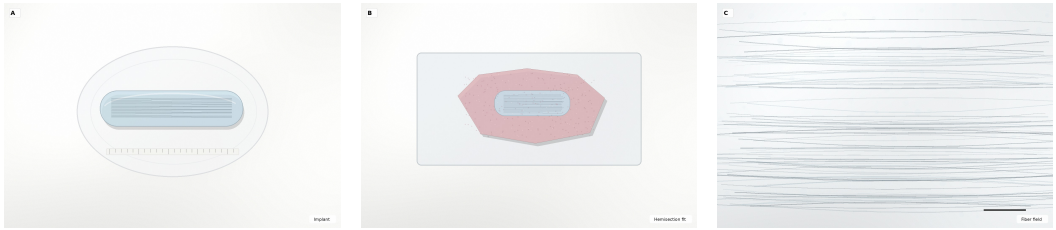

(a) Implant body **(b)** Lesion fit **(c)** Aligned field

Figure 1. Representative construct views.

It can be seen from the construction of the implant depicted in Figure 1 that the visual identity of the implant is provided by its hydrated cylindrical shape, the longitudinal fit into the hemisection, and the alignment of its internal fiber array. It is important to mention

that these particular figures were chosen to make the connection between the material characterization and the specific function of the construct in terms of repair.

Workflow panels in Figure 2 break the experiment down into three practical actions: scaffold construction, NSC compatibility and fate testing, and tissue-level endpoint collection. This placement explains the reason why the same scaffold is characterized based on material durability, cell reaction, histological repair, axon growth, and locomotor function and not by any one measurement alone.

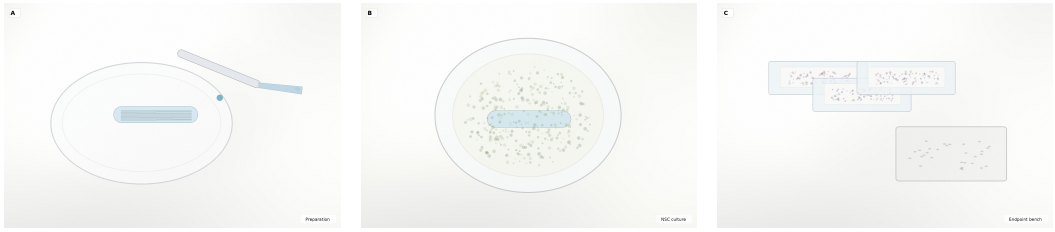

(a) Preparation **(b)** NSC culture **(c)** Tissue endpoints

Figure 2. Experimental workflow images.

This organization is critical because the biological interpretation of every endpoint differs depending on the moment in time when it was made. In vitro NSC culture results indicate whether the scaffold-drug system supports neuron-specific markers, but this does not indicate either lesion healing or improvement in locomotion. Histology reveals how the repaired tissue is arranged within the spinal cord, but by itself this does not prove that the hindlimbs can move in concert. Therefore, every measurement is connected with the correct level of generalization. Scaffold preparation is associated with material reproducibility, cell culture with the cytocompatibility and fate reaction, and endpoint measurements with an overall animal effect. Thus, using this workflow, the manuscript avoids confusing in vitro results with animal results.

2.2. Calculations for drug-associated change

For each measurement, the drug-free scaffold group was compared with the WAY-316606-loaded scaffold group. When a higher value indicated improvement, the scaffold-to-drug increment was calculated as

$$D_i^+(\%) = 100 \times \frac{x_{\mathrm{W+S},i} - x_{\mathrm{S},i}}{x_{\mathrm{S},i}}, \tag{1}$$

where $x_{\mathrm{S},i}$ is the drug-free scaffold value and $x_{\mathrm{W+S},i}$ is the value for the WAY-316606-loaded scaffold. This calculation reports the percentage change produced by adding WAY-316606 to the same scaffold design.

For measurements in which a lower value indicated improvement, such as cavity area or GFAP burden, the direction was reversed:

$$D_i^-(\%) = 100 \times \frac{x_{\mathrm{S},i} - x_{\mathrm{W+S},i}}{x_{\mathrm{S},i}}. \tag{2}$$

This expression keeps all reported increments in the favorable direction. A positive value therefore means that the WAY-316606-loaded scaffold performed better than the drug-free scaffold, even when the raw measurement decreased.

A second calculation estimated the fraction of the final favorable change that was associated with adding WAY-316606 after the scaffold effect was present. For higher-is-better measurements, this fraction was calculated as

$$F_i^+(\%) = 100 \times \frac{x_{\mathrm{W+S},i} - x_{\mathrm{S},i}}{x_{\mathrm{W+S},i} - x_{\mathrm{U},i}}, \tag{3}$$

where $x_{U,i}$ denotes the untreated SCI value or the control-cell value. For lower-is-better measurements, the fraction was calculated as

$$F_i^{-}(\%) = 100 \times \frac{x_{S,i} - x_{W+S,i}}{x_{U,i} - x_{W+S,i}}. \quad (4)$$

The denominator refers to the total distance between the untreated and drug-loaded conditions. The numerator reflects the gain made in this distance when WAY-316606 is added to the scaffold. This type of calculation is a descriptive measure used to find out which biological measurements are the most sensitive to the drug addition step.

These two calculations have different purposes. In the first case, the calculation reveals what gain is achieved when adding the drug in relation to the drug-free scaffold group. It may be important if one wants to know whether there is any additional effect of the drug after the material bridge has been established. The second calculation is about the following question: how much of the favorable distance between the untreated and drug-loaded groups is due to the drug step as opposed to the scaffold step? These two calculations are not meant to provide mechanistic evidence, but rather they allow comparing biological measurements with diverse units and meanings.

3. Results

3.1. Material stability and viability of NSC

The scaffold was degrading gradually through eight weeks of observation period. The weight loss of the scaffold was 5.08% at two weeks, 9.24% at four weeks, 16.49% at six weeks, and 22.53% at eight weeks. The same material window remained compatible to NSCs, the viability was $81.45 \pm 0.58\%$ and $77.61 \pm 4.26\%$ for the drug-free scaffold on days 1 and 3, respectively, and $84.14 \pm 2.38\%$ and $81.54 \pm 2.17\%$ for the WAY-316606-loaded scaffold.

Table 2. Material and viability values.

Measurement	2 weeks	4 weeks	6 weeks	8 weeks
Scaffold weight loss (%)	5.08	9.24	16.49	22.53

Measurement	Scaffold	WAY-316606 + Scaffold
NSC viability, day 1 (%)	81.45 ± 0.58	84.14 ± 2.38
NSC viability, day 3 (%)	77.61 ± 4.26	81.54 ± 2.17

These values demonstrate that WAY-316606 loading did not affect NSC viability in early stages. The scaffold with drugs showed slightly increased viability at both time points, but the key thing here is no decrease in viability that would have demonstrated lack of cytocompatibility. This is important since the changes in the proportions of $MAP2^{+}$, $NeuN^{+}$, or $GFAP^{+}$ will be more convincing if the survival is in acceptable limits.

Degradation numbers also confirm that the construct did not dissolve quickly during the time when the events related to repair processes took place. While 5.08% weight loss after two weeks suggests preservation of its structure in the early stages, 22.53% loss after eight weeks indicates gradual remodeling, but not short-term stability. In terms of using this material as the spinal cord implant, such behavior is optimal since too quick dissolution removes the guiding structure before the proper organization of the tissues occurs, and too slow – does not allow the integration with host lesions. Thus, the obtained results support using the scaffold as a guiding structure temporarily rather than as a long-lasting space filler.

The viability comparison is as important, as the difference between day-1 and day-3 values in the WAY-316606 loaded construct group is more than 81%. The difference between the scaffold group and WAY-316606-loaded group could not be interpreted as the confirmation of the role of WAY-316606 as the factor increasing cell survival; the numbers should be viewed as the proof that 10 μg dosage did not impose additional toxic effect on

NSCs. Such interpretation is quite conservative and consistent with the general aim of this study. The further discussion of changes in neuronal and glial markers will relate to change of phenotype and tissue quality.

The images shown in Figure 3 depict the results of both material and viability tests as a compatibility check. As for the degradation series, it is related to the progressive increase in scaffold weight loss from 5.08% to 22.53% during eight weeks. Moreover, as for the cell-field pairs, they represent the preservation of NSC compatibility in two different scaffold groups. In case of WAY-316606-loaded scaffold, since the day-1 and day-3 viability exceeded 81%, there is no necessity to take into account any toxicity at the first stages.

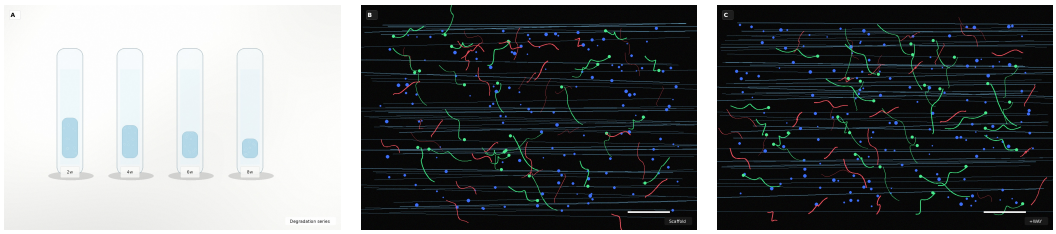

(a) Mass loss **(b)** Scaffold **(c)** +WAY

Figure 3. Material persistence and NSC compatibility.

3.2. Neuronal lineage response

The largest effect associated with the application of drugs was seen in the neuronal lineage markers. $MAP2^+$ cells were increased from $32.24 \pm 0.79\%$ in control culture to $40.02 \pm 4.88\%$ in the scaffold group and $63.37 \pm 3.47\%$ in WAY-316606-loaded scaffold group. $NeuN^+$ cells were increased from $31.50 \pm 2.73\%$ to $44.51 \pm 5.48\%$ and further to $59.79 \pm 2.99\%$. There were astrocytes differentiated oppositely, with the decrease of the percentage of $GFAP^+$ cells from $83.22 \pm 2.15\%$ in control culture to $68.15 \pm 3.48\%$ in WAY-316606-loaded scaffold group.

The numbers in Table 3 clearly indicate that WAY-316606 affects the cellular phenotype stronger than it affects early viability. Even though the scaffold itself increased $MAP2^+$ and $NeuN^+$ fractions, the drug-induced change was much bigger: $MAP2^+$ cells went up by 58.3%, and $NeuN^+$ cells increased by 34.3% compared to the drug-free scaffold. These results confirm that SFRP1 inhibition targets Wnt-responsive neuronal differentiation rather than simply being a material-filling drug [22].

Table 3. NSC marker response.

Measurement	Control	Scaffold	WAY-316606 + Scaffold
$GFAP^+$ cells (%)	83.22 ± 2.15	–	68.15 ± 3.48
$MAP2^+$ cells (%)	32.24 ± 0.79	40.02 ± 4.88	63.37 ± 3.47
$NeuN^+$ cells (%)	31.50 ± 2.73	44.51 ± 5.48	59.79 ± 2.99

Lineage table represents one of the strongest pieces of evidence that the effect of the drug is not restricted to material filling. MAP2 is associated with a cytoskeletal state corresponding to neuronal differentiation, whereas NeuN corresponds to the neuronal phenotype. Hence, the increase in both markers shows that the effect is not restricted to just one stage of neuronal development. In addition, the absence of the value of a drug-free scaffold for GFAP in the table does not allow us to calculate the increase in this marker from the scaffold to the drug-loaded scaffold, but we can still say that the fraction of astroglia is smaller for the construct containing the drug. All of these markers provide support for the shift away from the astroglia-dominated state towards a neuron-enriched state.

In particular, the extent of MAP2 increase is critical. It rose from $40.02 \pm 4.88\%$ for the scaffold group to $63.37 \pm 3.47\%$ for the drug-loaded group, i.e., the relative increase was 58.3%. It was higher than the change in day-3 viability, thus the result cannot be explained by the change in cell survival. In a similar fashion, NeuN increased from $44.51 \pm 5.48\%$ to

59.79 ± 2.99%. Combined increase in MAP2 and NeuN supports the view that WAY-316606 enhances the neuronal nature of cell response inside the scaffold environment.

The three fields in Figure 4 serve as a visual illustration for the marker values in Table 3. The control group continues to be dominated by astroglial signal, the scaffold group is partially enriched by neurons, and the WAY-316606-loaded scaffold group demonstrates the greatest transition towards a neuronally enriched lineage appearance. Thus, the presented panel sequence confirms the idea that WAY-316606's influence on cell fate is primarily numerically demonstrated.

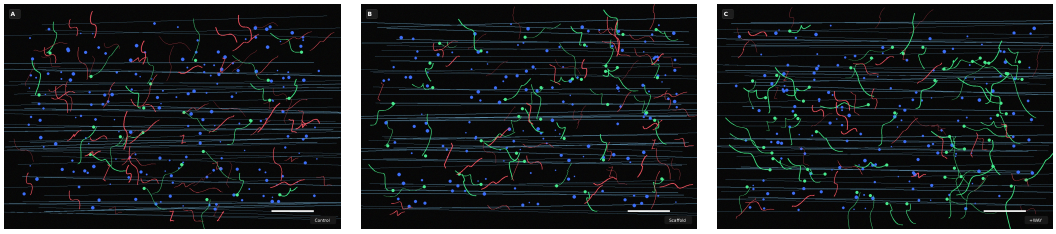

(a) Control **(b)** Scaffold **(c)** +WAY

Figure 4. NSC fate fields.

This cellular evidence provides a basis for the biological effect that the animal data has to show. If WAY-316606's effect was limited to an increase in the NSCs markers expression in vitro and could not improve the GFAP burden or the density of neurons in vivo, it would mean nothing more than the cell culture effect. Otherwise, if the in vivo data indicated only the effect of cavity closing without neuronal markers enrichment, the effect of the drug would be rather weak. Therefore, the figure on cell lineage illustrates the phenotype effect which should be observed in the lesion afterwards due to the biological relevance of the drug action.

3.3. Lesion remodeling, neuron tissue density, and GFAP burden

Tissue-level repair was dissociated from structural closure into cellular quality. The cavity size was reduced from 0.37 ± 0.08 mm^2 in untreated SCI group to 0.06 ± 0.006 mm^2 for the scaffold and 0.05 ± 0.006 mm^2 for the WAY-316606-loaded scaffold. The results suggest that most of the gross lesion reduction has been provided by the scaffold itself. Nissl bodies had an opposite trend, increasing from 6.0 ± 0.4 mm^{-2} in untreated SCI group to 35.8 ± 1.1 mm^{-2} for the scaffold and 50.5 ± 1.9 mm^{-2} for the WAY-316606-loaded scaffold.

GFAP burden demonstrated the advantage of the WAY-316606-loaded scaffold. At the lesion edge, the GFAP value dropped from 18.70 ± 1.43% in untreated SCI to 10.62 ± 2.98% for the scaffold and 7.19 ± 1.26% for the drug-loaded scaffold. In the lesion core, the GFAP value decreased from 16.75 ± 2.14% to 11.28 ± 1.10% and finally to 6.02 ± 0.91%. This is important due to the fact that glial scarring plays a dual role, being a protecting factor and an inhibitor at the same time; the goal of the treatment is achieving the modulation of the excessive GFAP burden rather than the complete removal of the boundary function of the astrocyte cells [23].

Separating the lesion-edge and lesion-core GFAP values is beneficial due to the fact that the two compartments have their own biological significance. The lesion edge is the interface zone between injured and spared tissue, where the boundary of the lesion is formed by the astrocytes, and which protects the tissue from further inflammation. The lesion core is the central part of the lesion that needs to be filled or bridged in order to restore the neural continuity. The drop of the GFAP values in the lesion edge and core, accompanied by the increase of Nissl and NeuN values, indicates the change of the tissue balance instead of the displacement of astrocytic signal. The decrease of the GFAP value from 11.28 ± 1.10% to 6.02 ± 0.91% in the lesion core is particularly important as the core is the compartment where the implant has been placed.

Animal values shown in Table 4 indicate that cavity size alone is inadequate as an indicator of repair quality. The drug-free scaffold has reduced cavity size by more than fivefold on its own, whereas WAY-316606 added only a modest improvement to the reduction in cavity area. On the other hand, the drug-loaded scaffold contributed substantially more in terms of the additional changes in Nissl density, GFAP reduction, and in vivo $NeuN^+$ density. It appears, thus, that the effect of WAY-316606 consists mostly of altering tissue composition.

Table 4. Animal repair values.

Measurement	Untreated SCI	Scaffold	WAY-316606 + Scaffold
Cavity area (mm^2)	0.37 ± 0.08	0.06 ± 0.006	0.05 ± 0.006
Nissl bodies (mm^{-2})	6.0 ± 0.4	35.8 ± 1.1	50.5 ± 1.9
GFAP at lesion edge (%)	18.70 ± 1.43	10.62 ± 2.98	7.19 ± 1.26
GFAP in lesion core (%)	16.75 ± 2.14	11.28 ± 1.10	6.02 ± 0.91
Axon growth distance (mm)	1.45 ± 0.18	2.83 ± 0.10	3.12 ± 0.23
$NeuN^+$ cells in vivo (mm^{-2})	18.33 ± 4.37	39.71 ± 1.63	61.25 ± 5.62
BBB score at 8 weeks	12.4 ± 0.3	16.5 ± 0.7	18.4 ± 0.5

This alters the interpretation of the whole experiment in vivo. Based on cavity area, the contribution of the drug would be rather modest, since scaffold on its own reduced the lesion size from 0.37 ± 0.08 mm^2 to 0.06 ± 0.006 mm^2. The neuronal and glial markers, however, present a quite different picture. Thus, Nissl bodies increased from 35.8 ± 1.1 mm^{-2} to 50.5 ± 1.9 mm^{-2}, and in vivo $NeuN^+$ density increased from 39.71 ± 1.63 mm^{-2} to 61.25 ± 5.62 mm^{-2}. The drug-loaded scaffold, then, did not reduce the cavity size, but increased neuronal enrichment of the repaired tissue.

What is even more important is that drug effect is not limited to a single marker. Thus, GFAP decreased in both compartments of the lesion, Nissl density increased, $NeuN^+$ density increased, distance of axonal growth increased, and BBB score increased. Since all of this happens in the same direction on tissue composition, continuity, and behavior, it increases credibility of the result. While data presented in table form are means for groups, the biological story is coherent: scaffold provides the geometric closure of the lesion, while WAY-316606 adds tissue quality.

The images in Figure 5 put the variables cavity size, Nissl stain intensity, and GFAP burden on a visual continuum. The scaffold group has the greatest degree of gross defect reduction, while the WAY-316606-loaded condition has an increased neuronal tissue staining and reduced GFAP associated rim. This visual separation corresponds to the trend seen quantitatively in Table 4, where structural filling has occurred in the scaffold group while the drug has mainly enhanced the cellular composition of the tissue field.

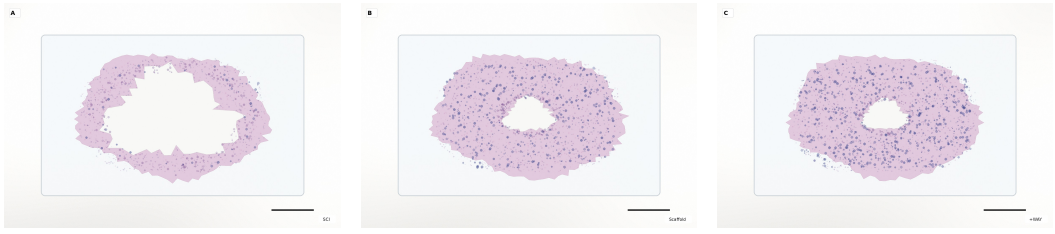

(a) SCI **(b)** Scaffold **(c)** +WAY

Figure 5. Lesion tissue appearance.

The progression of images from SCI, to scaffold, and then to WAY-316606-loaded scaffold helps illustrate the spatial concept better than any numeric representation. The first image of SCI represents a lesion field characterized by high central cavity defect and surrounding reaction fields. The scaffold image reflects reduction of the defect, in line with the bridging role played by PCL/ASCM/G-CD-PEGDA. The WAY-316606-loaded scaffold image preserves the benefit of structure while exhibiting a tissue field more characteristic

of neuronal tissue filling and reduced GFAP burden. It is important for the visual representation to be made since it ensures the response of the drug cannot be interpreted as mere scaffold filling.

Finally, the lesion figure reinforces the reasoning behind the cautious use of GFAP data. The reduction in GFAP signal intensity is desirable when it accompanies improvements in neuronal tissues measurements. In this case, lesion-edge and lesion core GFAP reduction has been accompanied by an increase in Nissl bodies as well as increased $NeuN^+$ cells density. It thus means there is a more balanced repair environment rather than suppression of astrocyte function. This conclusion is based on current knowledge on the role of astrocytes in protecting neurons following SCI [5,23].

3.4. Axonal growth and locomotor recovery

The distance of axon growth was raised from 1.45 ± 0.18 mm in untreated SCI to 2.83 ± 0.10 mm in the scaffold condition and 3.12 ± 0.23 mm in the WAY-316606-loaded scaffold condition. Density of $NeuN^+$ cells increased from 18.33 ± 4.37 mm^{-2} to 39.71 ± 1.63 mm^{-2} and to 61.25 ± 5.62 mm^{-2}. Locomotor performance in the open field improved in the same direction: eight-week BBB score was raised from 12.4 ± 0.3 in the untreated SCI to 16.5 ± 0.7 with the scaffold and 18.4 ± 0.5 with the drug-loaded scaffold. The BBB scale is a sensitive measure of locomotion in rats and is frequently employed to estimate the recovery of the hindlimbs after SCI [24].

The degree of locomotion improvement was less than the change in density of mature neurons. The discrepancy is biologically realistic, since locomotion requires the presence of intact tracts, synaptic integration, conduction, circuitry at the level of the lesion, and compensatory mechanisms, but not only neuronal marker density [25]. The information therefore supports the conclusion: WAY-316606 modifies the recovery trajectory, but the values suggest partial, rather than complete, spinal cord reconstruction.

The axon-growth result provides an important link between the histological and behavioral results. Growth distance was increased from 2.83 ± 0.10 mm with the scaffold to 3.12 ± 0.23 mm with the drug-loaded scaffold. The increase of 10.2% in the scaffold-to-drug condition is lower than the increase in MAP2, NeuN, and Nissl density, implying that axonal extension does not depend solely on the local environment of neuronal markers. It requires lesion navigation, interaction with inhibitory matrix and glial signals, and establishment of functional contacts. The result is therefore consistent with partial reconstruction, rather than full one.

The BBB improvement is similarly conservative. The score was increased from 12.4 ± 0.3 with the scaffold to 16.5 ± 0.7 and to 18.4 ± 0.5 with the drug-loaded scaffold. The additional 11.5% improvement is significant in that it occurred in the same direction as the increase in $NeuN^+$ density, axon growth distance, and decrease in GFAP burden. At the same time, the score does not imply recovery to the normal level. The behavioral result should therefore be interpreted as a support for the histological pattern, rather than evidence of the complete reconstruction of the spinal circuits.

The continuity panels in Figure 6 link the histological region of injury repair to the behavioral outcome measure. The SCI-only condition exhibits relatively poor bridging, the scaffold condition has more aligned axonal regions, while the WAY-316606-loaded condition exhibits the most significant continuity pattern. The open-field panel is arranged next to the axonal fields in order to highlight the fact that the interpretation of the BBB score is considered as a downstream function of what was observed at the tissue level.

The figure is designed as a recovery chain. In the axon panels there is increasing continuity in the lesion environment, while the open-field panel links the tissue observation to a behavioral aspect. The camera style presentation avoids the representation of the behavior as an isolated number which is not directly related to the histological findings. Rather the reader perceives that WAY-316606-loaded scaffold condition is accompanied by a series of observations, including increased neuronal density, low GFAP burden, greater

axonal length, and improved locomotion. The association is not one-to-one since the BBB score takes into account multiple neurological and musculoskeletal factors.

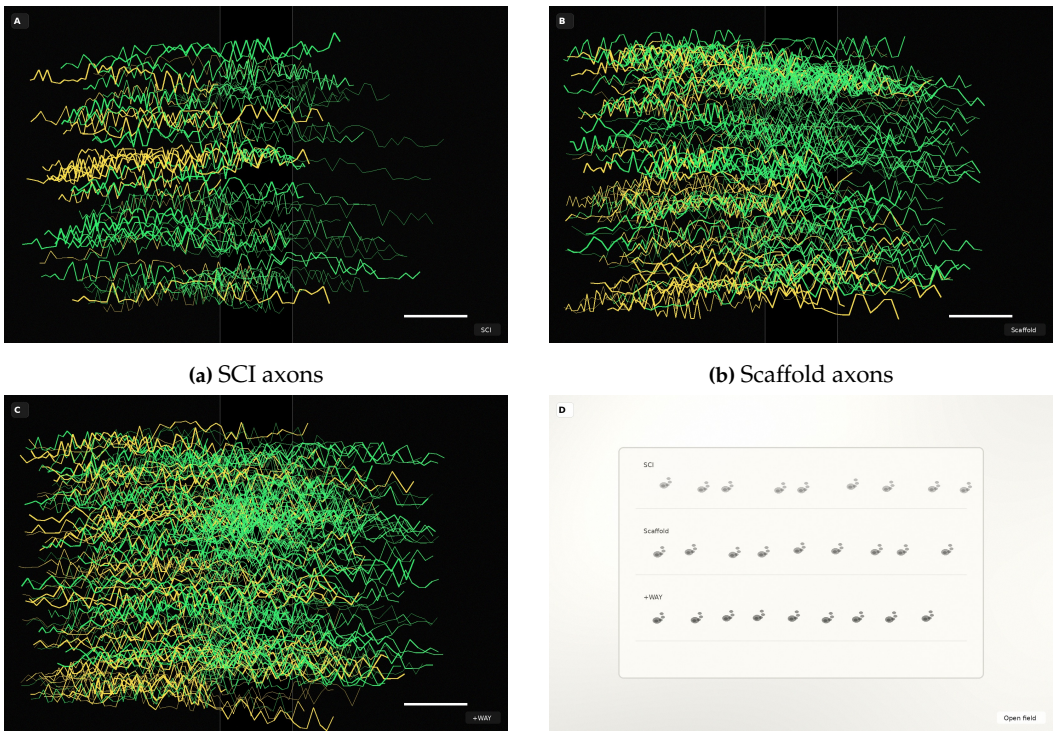

(a) SCI axons **(b)** Scaffold axons

(c) +WAY axons **(d)** Open field

Figure 6. Neural continuity and locomotor readout.

The increments shown in Table 5 represent the most direct numerical response to the objective of this study. The largest WAY-316606 fraction belongs to $MAP2^+$ differentiation, in vitro $NeuN^+$ maturation, in vivo $NeuN^+$ density, and lesion-core GFAP reduction. Cavity area has the smallest fraction at 3.1%, reaffirming the observation of scaffold-dependent closure of gross lesion geometry. Such a hierarchy suggests a predominantly biological effect of the drug, specifically in the context of neural differentiation and glial moderation, and not simply as a filler of the defect.

Table 5. WAY-associated increments.

Measurement	Scaffold-to-drug increment (%)	WAY fraction of final change (%)
$MAP2^+$ cells	58.3 increase	75.0
$NeuN^+$ cells in vitro	34.3 increase	54.0
Cavity area	16.7 reduction	3.1
Nissl bodies	41.1 increase	33.0
GFAP at lesion edge	32.3 reduction	29.8
GFAP in lesion core	46.6 reduction	49.0
Axon growth distance	10.2 increase	17.4
$NeuN^+$ cells in vivo	54.2 increase	50.2
BBB score	11.5 increase	31.7

The order of these increments is far more meaningful than their respective percentages. Specifically, $MAP2^+$ cells exhibited the highest WAY-316606 fraction at 75.0%, followed by in vitro $NeuN^+$ cells at 54.0%, in vivo $NeuN^+$ density at 50.2%, and lesion-core GFAP reduction at 49.0%. In other words, these numbers indicate what biological processes were the most responsive to the addition of WAY-316606 on top of the scaffold. As for cavity area, its WAY-316606 fraction equaled a mere 3.1%, and this is the endpoint demonstrating that

the geometry of the defect had already been largely solved with the help of the material bridge.

This endpoint summary in Figure 7 is a synthesis of the same conclusion that was arrived at using Table 5. Cavitation of the structure, which is achieved mainly by the scaffold, is used as an anchor to describe the structural part of the experiment while neuronal density, GFAP regulation, and enhanced locomotor ability are biological advantages of WAY-316606 delivery. These panels are then referenced as the ultimate answer to the experiment question posed earlier.

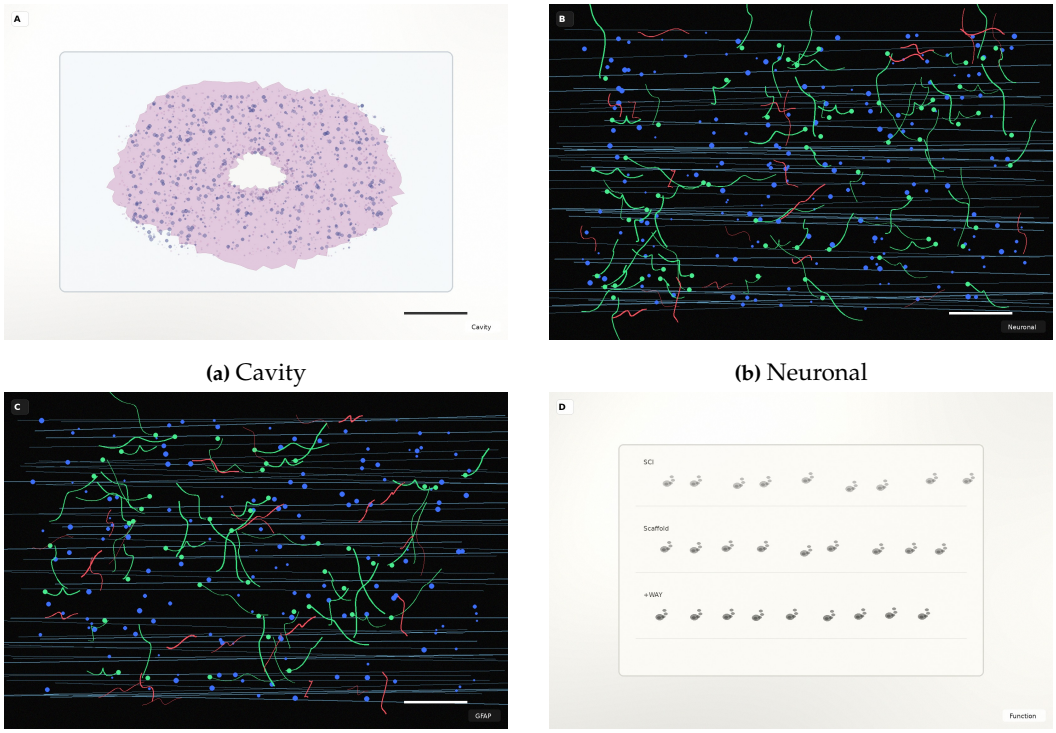

(a) Cavity **(b)** Neuronal

(c) GFAP **(d)** Function

Figure 7. Endpoint-level repair profile.

4. Discussion

The set of integrated endpoints presented in Figure 7 provides a natural separation between material-related and drug-affected repair parameters. The aligned PCL/ASCM/G-CD-PEGDA scaffold acts as a framework for the lesion closure, while WAY-316606 influences cell quality. Such differentiation is important since biomaterial studies of SCI repair may look extremely successful in terms of cavity area reduction despite a lack of neuronal markers, gliosis and no functional improvement. The current data show that the drug-impregnated scaffold improves several repair parameters at the same time: neuronal differentiation, increase of mature-neuron associated density, GFAP burden reduction, increase of axonal extension length and BBB score.

Biocompatibility of the material provides a good basis for the biological interpretation. The viability of NSCs in the WAY-316606-loaded scaffold was not decreased on day 1 and day 3. A cytotoxic or poorly tolerated composition may lead to misinterpretation of the marker proportion, since some cells are more sensitive to stress than others and die preferentially. In the current experiment, early viability stayed above 81% for both studied days in the drug-loaded group, thus, the later increase in $MAP2^+$ and $NeuN^+$ cells is probably caused by the phenotype change rather than cell death selection. This is in agreement with the common role of hydrogel materials as hydrated matrices for neurorepair [26,27].

Scaffold design explains the high effectiveness of cavity closure in both implantation groups. The aligned PCL fibers may serve as directional guidance components, and ASCM

may provide tissue-derived extracellular matrix signals. The combination of such features is optimal for the anisotropic nature of spinal cord tissue, where filling is less desired and longitudinal repair is preferable. The studies of direct writing and near-field fiber fabrication confirm that scaffold design may influence cell alignment and tissue patterning rather than serve as pure mechanical scaffold [9,10,12]. Low WAY-316606 fraction for cavity area is not a negative property of the drug but rather evidence of the effectiveness of the material component in the cavity closing.

The largest impact of the drug was observed in neuronal lineages and mature neurons-associated tissue. $MAP2^+$ cells increased in 58.3% with respect to scaffold implantation, while in vivo density of $NeuN^+$ cells increased in 54.2%. Such changes are expected biologically for SFRP1 inhibition, since the local reduction in the activity of Wnt/β-catenin signaling that regulates stem cell proliferation and neuronal differentiation is expected under such conditions [17,18]. The data do not require the assumption about the universal positive effect of Wnt signaling in the case of SCI; instead, it demonstrates that the local WAY-316606 delivery in the current scaffold coincided with the stronger outcomes for neuronal markers.

GFAP outcomes need a precise interpretation. Astrocytes play a role in the wound containment and inhibiting scar formation after SCI [5,23]. The desirable outcome is not the disappearance of astrocytes but the decrease in their GFAP burden together with the improvement of neuronal markers. The WAY-316606-loaded scaffold satisfies this condition: GFAP decreased from 10.62% to 7.19% in the lesion edge and from 11.28% to 6.02% in the lesion core, comparing with drug-free scaffold, while Nissl bodies and $NeuN^+$ density increased. Such paired trend shows the development of the repair phenotype that is less gliotic and neuronally enriched.

Functional recovery correlated with tissue markers but remained appropriate. BBB score was increased from 16.5 ± 0.7 for the scaffold group to 18.4 ± 0.5 for the WAY-316606-loaded scaffold, providing 11.5% improvement. The increase is significant due to the correlation with better histology and neuronal markers but not complete restoration. Locomotor behavior combines supraspinal control, segmental circuitry, spared fibers, synapses connections, muscle tone and compensation [24,25]. A moderate improvement in locomotion is thus consistent with the effective but incomplete tissue repair.

The study has definite limitations. Calculations are based on the group-level numerical values, thus, animal-level covariance and additional statistical modeling cannot be provided. No exact quantitative values were assigned to the pathway images unless it is possible numerically. The long-term durability of the effects, electrophysiological reconnections, dose response for WAY-316606 and its release kinetics need additional analysis. Such limitations do not change the main conclusion but only specify the level of it.

5. Conclusion

The combination of aligned PCL/ASCM/G-CD-PEGDA with WAY-316606 promotes spinal cord regeneration by way of complimentary roles from both the structural and the biological sides. The role of the scaffold is primarily in gross lesion cavity closure and serves as a cytocompatible platform during eight weeks of regeneration. The introduction of WAY-316606 makes the process more efficient in neuronal differentiation, with the increase of Nissl body and $NeuN^+$ cell density, reduction of GFAP load, and axonal growth and BBB score elevation. It can be clearly stated that WAY-316606 works primarily by improving the neuronal and glial tissue quality inside the regenerated area rather than by further lesion cavity closure.

The numerical results confirm the answer at each level of measurements. The loss of weight from 5.08% at two weeks to 22.53% at eight weeks demonstrates that the scaffold stays in place with a gradual remodeling. The viability of NSCs over 77% in both scaffold groups shows that the scaffold and the drug-loaded one are compatible with early survival. The increase in $MAP2^+$ and $NeuN^+$ demonstrates the positive effect of WAY-316606 on the development of neurons in the scaffold environment. In vivo numbers show the same

effect in the injured cord: Nissl density and $NeuN^+$ density increase and GFAP burden decreases both at lesion edge and lesion core. Further, the axon-growth distance and BBB score prove that the histological changes lead to connectivity and functional improvement.

Thus, the interpretation becomes very specific. The aligned PCL/ASCM/G-CD-PEGDA serves as the physical scaffold through which repair takes place while WAY-316606 inhibits SFRP1 and promotes neuronal markers. The scaffold closes and organizes the cavity; the drug enhances the repair zone for neurons and reduces astroglial response. These roles explain the low influence of WAY-316606 on the cavity area and the high contribution of WAY-316606 to MAP2, NeuN, Nissl and lesion-core GFAP. Further work will need to find the WAY-316606 release kinetics, check several concentrations, measure the electrophysiological conduction recovery across the scaffold and the persistence of neuronal and glial tissue quality improvements beyond eight weeks.

References

[1] Ahuja, C. S., Wilson, J. R., Nori, S., Kotter, M., Druschel, C., Curt, A., & Fehlings, M. G. (2017). Traumatic spinal cord injury. Nature reviews Disease primers, 3(1), 17018.

[2] Tran, A. P., Warren, P. M., & Silver, J. (2018). The biology of regeneration failure and success after spinal cord injury. Physiological reviews, 98(2), 881-917.

[3] Venkatesh, K., Ghosh, S. K., Mullick, M., Manivasagam, G., & Sen, D. (2019). Spinal cord injury: pathophysiology, treatment strategies, associated challenges, and future implications. Cell and tissue research, 377(2), 125-151.

[4] O'Shea, T. M., Burda, J. E., & Sofroniew, M. V. (2017). Cell biology of spinal cord injury and repair. The Journal of clinical investigation, 127(9), 3259-3270.

[5] Bradbury, E. J., & Burnside, E. R. (2019). Moving beyond the glial scar for spinal cord repair. Nature communications, 10(1), 3879.

[6] Perale, G., Rossi, F., Sundstrom, E., Bacchiega, S., Masi, M., Forloni, G., & Veglianese, P. (2011). Hydrogels in spinal cord injury repair strategies. ACS chemical neuroscience, 2(7), 336-345.

[7] Haggerty, A. E., & Oudega, M. (2013). Biomaterials for spinal cord repair. Neuroscience bulletin, 29(4), 445-459.

[8] Führmann, T., Anandakumaran, P. N., & Shoichet, M. S. (2017). Combinatorial therapies after spinal cord injury: how can biomaterials help?. Advanced healthcare materials, 6(10), 1601130.

[9] Chen, H., Malheiro, A. D. B. F. B., van Blitterswijk, C., Mota, C., Wieringa, P. A., & Moroni, L. (2017). Direct writing electrospinning of scaffolds with multidimensional fiber architecture for hierarchical tissue engineering. ACS Applied Materials & Interfaces, 9(44), 38187-38200.

[10] He, F. L., Li, D. W., He, J., Liu, Y. Y., Ahmad, F., Liu, Y. L., ... & Yin, D. C. (2018). A novel layer-structured scaffold with large pore sizes suitable for 3D cell culture prepared by near-field electrospinning. Materials Science and Engineering: C, 86, 18-27.

[11] Fuh, Y. K., Wu, Y. C., He, Z. Y., Huang, Z. M., & Hu, W. W. (2016). The control of cell orientation using biodegradable alginate fibers fabricated by near-field electrospinning. Materials Science and Engineering: C, 62, 879-887.

[12] Park, Y. S., Kim, J., Oh, J. M., Park, S., Cho, S., Ko, H., & Cho, Y. K. (2019). Near-field electrospinning for three-dimensional stacked nanoarchitectures with high aspect ratios. Nano letters, 20(1), 441-448.

[13] Liu, J., Chen, J., Liu, B., Yang, C., Xie, D., Zheng, X., ... & Jin, D. (2013). Acellular spinal cord scaffold seeded with mesenchymal stem cells promotes long-distance axon regeneration and functional recovery in spinal cord injured rats. Journal of the neurological sciences, 325(1-2), 127-136.

[14] Chen, J., Zhang, Z., Liu, J., Zhou, R., Zheng, X., Chen, T., ... & Jin, D. (2014). Acellular spinal cord scaffold seeded with bone marrow stromal cells protects tissue and promotes functional recovery in spinal cord-injured rats. Journal of neuroscience research, 92(3), 307-317.

[15] Wang, Y. H., Chen, J., Zhou, J., Nong, F., Lv, J. H., & Liu, J. (2017). Reduced inflammatory cell recruitment and tissue damage in spinal cord injury by acellular spinal cord scaffold seeded with mesenchymal stem cells. Experimental and therapeutic medicine, 13(1), 203-207.

[16] Ban, D. X., Liu, Y., Cao, T. W., Gao, S. J., & Feng, S. Q. (2017). The preparation of rat's acellular spinal cord scaffold and co-culture with rat's spinal cord neuron in vitro. Spinal cord, 55(4), 411-418.

[17] Li, X., Fan, C., Xiao, Z., Zhao, Y., Zhang, H., Sun, J., ... & Dai, J. (2018). A collagen microchannel scaffold carrying paclitaxel-liposomes induces neuronal differentiation of neural stem cells through Wnt/β - catenin signaling for spinal cord injury repair. Biomaterials, 183, 114-127.

[18] Gao, J., Liao, Y., Qiu, M., & Shen, W. (2021). Wnt/β - catenin signaling in neural stem cell homeostasis and neurological diseases. The Neuroscientist, 27(1), 58-72.

[19] Hawkshaw, N. J., Hardman, J. A., Haslam, I. S., Shahmalak, A., Gilhar, A., Lim, X., & Paus, R. (2018). Identifying novel strategies for treating human hair loss disorders: cyclosporine A suppresses the Wnt inhibitor, SFRP1, in the dermal papilla of human scalp hair follicles. PLoS biology, 16(5), e2003705.

[20] Donega, V., van der Geest, A. T., Sluijs, J. A., van Dijk, R. E., Wang, C. C., Basak, O., ... & Hol, E. M. (2022). Single-cell profiling of human subventricular zone progenitors identifies SFRP1 as a target to re-activate progenitors. Nature communications, 13(1), 1036.

[21] Ma, Q., Wang, S., Xie, Z., Shen, Y., Zheng, B., Jiang, C., ... & Jie, Z. (2020). The SFRP1 Inhibitor WAY-316606 Attenuates Osteoclastogenesis Through Dual Modulation of Canonical Wnt Signaling. Journal of Bone and Mineral Research, 37(1), 152-166.

[22] Liu, Y., Wang, X., Lu, C. C., Sherman-Kermen, R., Steward, O., Xu, X. M., & Zou, Y. (2008). Repulsive Wnt signaling inhibits axon regeneration after CNS injury. Journal of Neuroscience, 28(33), 8376-8382.

[23] Yang, T., Dai, Y., Chen, G., & Cui, S. (2020). Dissecting the dual role of the glial scar and scar-forming astrocytes in spinal cord injury. Frontiers in cellular neuroscience, 14, 78.

[24] Basso, D. M., Beattie, M. S., & Bresnahan, J. C. (1995). A sensitive and reliable locomotor rating scale for open field testing in rats. Journal of neurotrauma, 12(1), 1-21.

[25] Courtine, G., & Sofroniew, M. V. (2019). Spinal cord repair: advances in biology and technology. Nature medicine, 25(6), 898-908.

[26] Lv, Z., Dong, C., Zhang, T., & Zhang, S. (2022). Hydrogels in spinal cord injury repair: a review. Frontiers in bioengineering and biotechnology, 10, 931800.

[27] Lin, P. H., Dong, Q., & Chew, S. Y. (2021). Injectable hydrogels in stroke and spinal cord injury treatment: a review on hydrogel materials, cell–matrix interactions and glial involvement. Materials Advances, 2(8), 2561-2583.